



# Thymoquinone ameliorates oxidative damage and histopathological changes of developing brain neurotoxicity

Hamid A Saleh, Gamal S. Abd El-Aziz, Hesham N. Mustafa, Magdy El-Fark, Ahmed Mal, Majdah Aburas & Abdel Halim Deifalla


To cite this article: Hamid A Saleh, Gamal S. Abd El-Aziz, Hesham N. Mustafa, Magdy El-Fark, Ahmed Mal, Majdah Aburas & Abdel Halim Deifalla (2019): Thymoquinone ameliorates oxidative damage and histopathological changes of developing brain neurotoxicity, Journal of Histotechnology

To link to this article: <https://doi.org/10.1080/01478885.2019.1619654>



Published online: 24 Jul 2019.



Submit your article to this journal 



View Crossmark data 



## Thymoquinone ameliorates oxidative damage and histopathological changes of developing brain neurotoxicity

Hamid A Saleh<sup>a</sup>, Gamal S. Abd El-Aziz<sup>a</sup>, Hesham N. Mustafa<sup>a</sup>, Magdy El-Fark<sup>b</sup>, Ahmed Mal<sup>c</sup>, Majdah Aburas<sup>d</sup> and Abdel Halim Deifalla<sup>e</sup>

<sup>a</sup>Anatomy Department, Faculty of Medicine, King Abdulaziz University, Jeddah, Saudi Arabia; <sup>b</sup>Anatomy Department, Faculty of Medicine, Suez Canal University, Ismailia, Egypt; <sup>c</sup>Marine Biology Department, Faculty of Marine Sciences, King Abdulaziz University, Jeddah, Saudi Arabia; <sup>d</sup>Biological Sciences Department, Faculty of Sciences, King Abdulaziz University, Jeddah, Saudi Arabia; <sup>e</sup>Anatomy Department, Faculty of Medicine, Arabian Gulf University, Manama, Bahrain

### ABSTRACT

Lead (Pb) toxicity is known to be a chief environmental health issue, especially for pregnant women and young children. Today, the use of medicinal herbs in the treatment of many diseases and different toxic agents has become highly accepted due to their effectiveness and lower costs. Thymoquinone (TQ), which is extracted from *Nigella sativa* seeds, is a potent antioxidant and anti-inflammatory agent. This study was designed to explore the optional protectivity of TQ against maternal and fetal oxidative stress and brain damage induced by Pb administration. Pregnant rats were distributed into seven groups: control group, TQ group, DMSO group, two groups Pb-treated (160 and 320 ppm), and two groups Pb-treated (160 and 320 ppm) co-treated with TQ. Administration started from gestation day 1 (GD1) to day 20 (GD20) through oral gavage once daily. Lead administration caused a dose-dependent toxicity for both mothers and fetuses. Also, the histopathological assessment of the brains from Pb-treated groups showed marked alterations. Co-treatment of with TQ and Pb caused a significant decrease in Pb levels as compared with those treated with Pb alone and amelioration of histopathological changes in the brains. It was concluded that co-treatment of TQ along with gestational Pb exposure could mitigate the effects against Pb-induced maternal and fetal neurotoxicity.

### KEYWORDS

Lead; oxidative stress; brain; Thymoquinone; fetal toxicity

### Introduction

Lead exposure has been considered a major health problem for pregnant women which makes the fetus vulnerable to Pb toxicity which is known as lead developmental toxicity [1]. Despite its usefulness as a chemical component in multiple industries, Pb is a toxic heavy metal, causing various harmful effects on different systems of the body. Gestational Pb exposure produces toxic effects, such as teratogenesis, risk of low birth weight and reduced mental development [2]. Moreover, studies have proved that prenatal Pb exposure exerts neurotoxicity during the differentiation and end-stages of fetal brain development [3].

It has been described that the cerebrum was a vulnerable target to Pb because of low levels of enzymes which are responsible for defending cerebrum against oxidative stress and because of high myelin content, that increases the vulnerability to peroxidation [4]. Also, Liu and colleagues stated that Pb can interrupt the blood-brain barrier structure by damaging

glial and endothelial cells and disturbing the building of tight-junctions between barrier cells [5].

Lead can induce oxidative damage to cellular components involved in the production of reactive oxygen species (ROS). The mechanisms for Pb-induced oxidative stress may be either direct or indirect by increasing lipid peroxidation to levels that can disturb membrane functions, lipid metabolism, and the antioxidant defense systems in cells [6,7]. In addition, interruption of the prooxidant/antioxidant balance via excessive ROS production had a significant role in brain pathology [8]. It was also proven that Pb crosses the placenta, and there is a positive correlation between Pb levels in both maternal and umbilical cord blood [9].

Thymoquinone (TQ) (2-isopropyl-5-methyl-1,2-benzoquinone) is the main active component of *Nigella sativa* seeds. This herb belongs to the Ranunculaceae family frequently grown in the Middle East, Western Asia, and Mediterranean countries [10,11]. Thymoquinone was shown to have wide pharmacological effects such as antioxidant, anti-

inflammatory and immunomodulatory, antibacterial, antimutagenic and antigenotoxic activities [12,13]. Also, TQ was found useful in the treatment of various diseases such as cardiac, respiratory, urinary, and hepatic disorders [14,15]. Moreover, many recent studies have described the following neuropharmacological properties of TQ, i.e. anticonvulsant [16], antinociceptive [17], anxiolytic and antidepressant [18], and antipsychotic potential [19]. Also, TQ countered memory impairments and enhanced cognitive functioning [20] and alleviated neuropathy in an experimental diabetic model [21].

Nevertheless, the potential protective role of TQ in developmental neurotoxicity has not been clearly documented to date. Hence, this study was planned to investigate the protective role of TQ against maternal and fetal oxidative stress and cerebral damage induced by Pb administration.

## Material and methods

### Animals and experiment

Female Sprague-Dawley albino rats (mature nulliparous) weighing 190–220 g were obtained from the animal house at the university. This study was approved by the Unit of Biomedical Ethics and Research, Faculty of Medicine, King Abdulaziz University. Females were kept in separate metallic cages under standard temperature ( $24 \pm 2^\circ\text{C}$ ), humidity ( $55 \pm 5\%$ ), and lighting (12 h/12 h light/dark) conditions. They were fed a standard chow diet *ad libitum* with free access to water. After acclimatization for two weeks, mating was conducted by placing the females overnight in a cage of a singly housed male. Gestation was confirmed by positive identification of spermatozoa in a vaginal lavage smear, and the confirmation date was designated as gestation day 0 (GD0) [22]. Pregnant females were randomly divided into seven groups ( $n = 8$  rats per group)

Control group: females received deionized water ( $\text{DIH}_2\text{O}$ ) from GD1-GD20 of pregnancy through oral gavage.

TQ group: females received TQ (10 mg/kg b.w.) dissolved in 50% dimethyl sulfoxide DMSO (Cat# 67–68-5, MilliporeSigma, Burlington, MA, USA) in  $\text{DIH}_2\text{O}$  once a day from GD1-GD20 of pregnancy through oral gavage.

DMSO group: females received 50% DMSO in  $\text{DIH}_2\text{O}$  once a day from GD1-GD20 through oral gavage.

Pb160 group: females received 160 ppm of lead acetate (PbAc) once a day from GD1-GD20 through oral gavage.

Pb160 + TQ group: females received 160 ppm of PbAc and TQ (10 mg/kg b.w.) once a day from GD1-GD20 through oral gavage.

Pb320 group: females received 320 ppm of PbAc once a day from GD1-GD20 through oral gavage.

Pb320 + TQ group: females received 320 ppm of PbAc and TQ (10 mg/kg b.w.) once a day from GD1-GD20 through oral gavage.

A PbAc solution was prepared by dissolving this salt in  $\text{DIH}_2\text{O}$  at concentrations of 0.1% for 160 ppm, and 0.2% for 320 ppm (w/v) [23,24]. A subsequent amount of 5 N HCl was added to lead acetate solution to prevent the precipitation of lead salts.

### Assessment of pregnant rats and fetuses

Pregnant females in each group were observed daily throughout gestation for mortality, morbidity, and body-weight gain. On GD20 and under ether-anesthesia, blood samples were taken via cardiac puncture, centrifuged at 3,000 rpm for 15 min to separate the serum, which was stored at  $-80^\circ\text{C}$ . The abdomen was opened, gravid uterine horns were removed and weighed, uterine contents were examined to determine the number of corpora lutea, implantation sites, and resorptions (embryonic death). Also, the number and position of viable and dead fetuses were counted. Additionally, pre-implantation losses were calculated as  $\text{number of corpora lutea} - \text{number of implantations} \times 100 \div \text{number of corpora lutea}$ . All viable fetuses and placentas were then removed and weighed separately. Fetal crown-rump length, head length, and biparietal diameter were measured using a Vernier caliper and recorded. The cerebellum of mother and fetal brains were quickly extracted, weighed, and divided sagittally. For each brain, the right half was fixed in 10% neutral-buffered formalin (NBF) for histological and immunohistochemical studies, and the left half was frozen and stored at  $-70^\circ\text{C}$  for biochemical assays.

### Biochemical assay measuring Pb levels in brain tissues

Left halves of brains from mothers and fetuses from all groups were digested in concentrated nitric acid (100,441, Suprapur®  $\text{HNO}_3$  65% w/w, Merck-Millipore, Darmstadt, Germany) using a shaking water bath at  $60^\circ\text{C}$  for 30 min. After digestion, the solution was diluted (1:5 v/v) with  $\text{DIH}_2\text{O}$ . Lead levels were measured using a graphite furnace atomic absorption spectrophotometer (Perkin-Elmer Model 3030, Hopkinton, MA, USA). Results were reported as  $\mu\text{g Pb/dl}$  blood, and Pb levels in brain and placenta were reported as  $\mu\text{g/g}$  tissue weight [25].

### Biochemical assays

Left halves of the brains from mothers and fetuses in all groups were homogenized (10% w/v) in ice-cold 0.1 M sodium phosphate buffer (pH 7.4). The homogenate was centrifuged twice at 4,000 rpm for 15–20 min at 4°C, and the resultant supernatant was used for estimation of various biochemical assays. The lipid peroxidation (LPO) was estimated by determining the amount of malondialdehyde (MDA), which is formed by peroxidation of membrane lipids using a thiobarbituric acid-reactive substances (TBARS) (QuantiChrom™ TBARS Assay Kit, DTBA-100, BioAssay Systems, Hayward, CA, USA) [26]. The antioxidant enzyme activity in rat brains was evaluated by determining the superoxide dismutase (SOD) activity using a Superoxide Dismutase Assay Kit (706,002, Cayman Chemical, Ann Arbor, MI, USA), in which a tetrazolium salt is used to detect superoxide radicals generated by xanthine oxidase and hypoxanthine [27]. Catalase (CAT) activity was assayed according to the peroxidatic function of catalase using a Catalase Assay Kit (707,002, Cayman Chemical) [27]. Glutathione peroxidase (GPx) activity was assayed by coupling the enzyme procedure with glutathione reductase using a Glutathione Reductase Assay Kit (703,202, Cayman Chemical) [27].

### Histological preparation

Maternal and fetal brains from all experimental groups were fixed in NBF for 24 h, dehydrated in an ascending ethyl alcohol gradient (50%, 70%, 90%, and 95%) 30 min each change, 100% ethyl alcohol for 1 h (two changes), cleared in xylene for 1 h (two changes), infiltrated with paraffin at 60°C for 2 h then embedded in paraffin. Sections 5 µm thick were cut using a rotatory microtome (Shandon, Finesse 325, Thermo Fisher Scientific, Luton, England), and mounted on slides precoated with an egg albumin–glycerol adhesive. Sections were deparaffinized in xylene (three changes, 15 min each) and rehydrated through a descending alcohol gradient (100%, 90%, 70%) 5–10 min each change to water, stained with Harris hematoxylin (HHS16, MilliporeSigma) for 10 min, washed in tap H<sub>2</sub>O to ‘blue’ the nuclei. Sections were counterstained with eosin (Alcoholic Eosin Y 515, 3,801,615; Leica Biosystems Inc., Buffalo Grove, IL, USA) for 3–5 min. Coverslips were mounted on slides using Canada balsam (C1795, MilliporeSigma).

### Immunohistochemistry (IHC)

Immunostaining for glial fibrillary acidic protein (GFAP) in the astrocytes was done using the streptavidin-biotin-complex method. Anti-GFAP (Anti-glial fibrillary acidic

protein, mouse monoclonal, IgG, clone GA5, MAB3402, RRID: AB\_94844 MilliporeSigma) diluted 1:1000 was used for IHC staining. After sections were deparaffinized, antigen retrieval was done in a microwave oven (Quelle Versand, Furth, Germany) at 700 watts for 5 min in citrate buffer, pH 6 (Cat# C9999, MilliporeSigma). Slides were immersed in a 3% hydrogen peroxide in DIH<sub>2</sub>O for 10 min to remove endogenous peroxidase activity. Histostain-Plus IHC Kit, HRP, broad spectrum (859,043, Invitrogen, Carlsbad CA, USA) was used for the following steps. After a phosphate buffer saline (PBS) wash, the kit blocking serum was used to prevent non-specific protein staining. Sections were incubated a 4°C overnight with anti-GFAP. For negative control group sections, PBS was applied in place of anti-GFAP antibody. Following a PBS wash, the kit biotinylated secondary antibody, Streptavidin-HRP complex and 3,3′ diaminobenzidine (DAB) chromogen were applied, sections were counterstained with hematoxylin, dehydrated, cleared, and a cover glass mounted with Entellan® mounting media (107,960, MilliporeSigma). GFAP-positive (GFAP<sup>+</sup>) astrocytes had brown cell membranes and cytoplasm with blue nuclei.

### Image capture and quantitative morphometric analysis

All sections were examined with an Olympus BX53 microscope fitted with a DP73 camera (Olympus, Tokyo, Japan) [28].

For each stained section, 10 non-overlapping fields were measured for each parameter, a mean value was calculated, and analyzed with Image-Pro Plus v6 (Media Cybernetics Inc., Bethesda, Maryland, USA). ImageJ (National Institute of Health, Bethesda, MD, USA) was used to quantify cells, measure area % covered by cells and color intensity of GFAP expression in astrocytes located within the cerebral cortex. All morphometric measurements were done at 100x magnification [28].

For each calculation, the background was determined by manually adjusting the Image Pro Plus density window until only the GFAP<sup>+</sup> tissue was selected. Digital brightfield images were uploaded into the ImageJ software, the scale was set using a digital micrometer gauge which converted pixel measurements to micrometers (µm) for all images. Cells were counted using the ImageJ cell-counter plug-in. After a grid was applied across the image, the number of different cell types were counted in the image. After establishing the color threshold, the total number of cells, area% covered by cells and average cell size were calculated using the automated cell-counter. Blood vessels expressing GFAP, nonspecific staining, and artifacts were ruled out before quantitation. When a subfield was too large to be

analyzed at one time, several measurements from adjacent non-overlapping areas were made and averaged. For the whole cortex, the GFAP<sup>+</sup> area was divided by the total area analyzed to obtain an estimate of area% occupied by astrocytes and their processes [28].

GFAP Area % = GFAP-positive area ÷ total area analyzed.

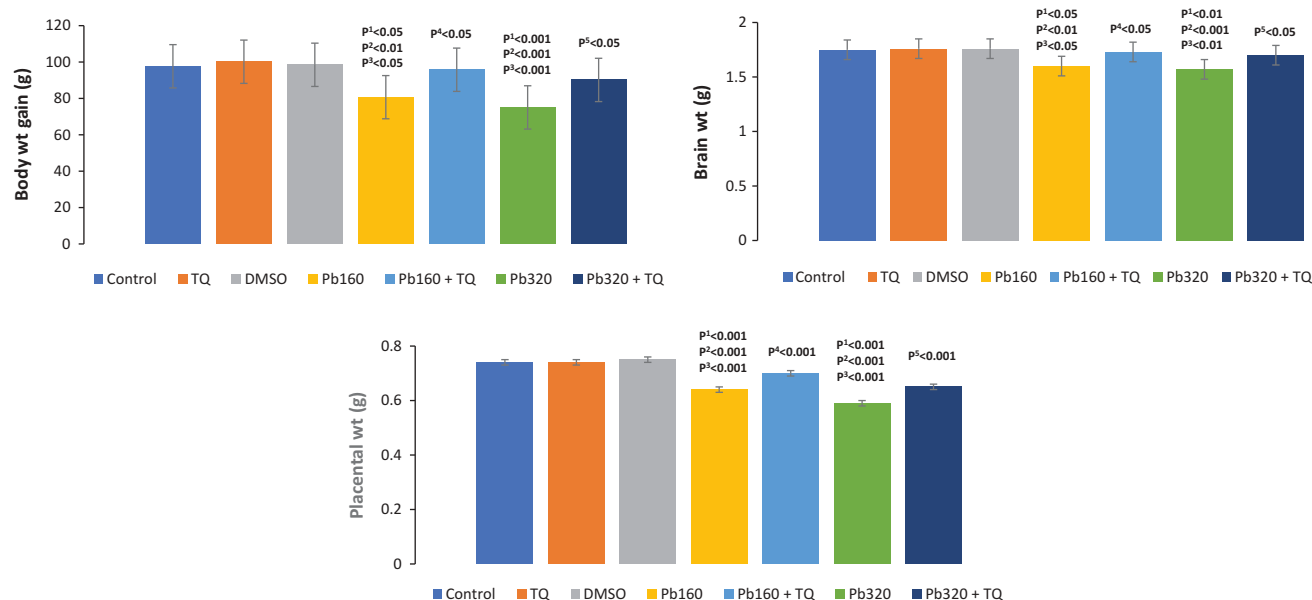
### Statistical analysis

All studied parameters of the different groups were presented as mean ± standard deviation. Data were analyzed using a one-way analysis of variance (ANOVA) followed by Bonferroni's *post hoc* test or Student's t-test, wherever applicable. All statistical analyses were done with IBM SPSS Statistics for Windows (Released 2015, Version 23.0, IBM Corp., Armonk, NY, USA). The values of  $P < 0.05$  were considered significant.

## Results

### Maternal results

During the experiment, two pregnant mothers from the Pb320-treated group died. Their post-mortem inspection revealed the fetuses had either aborted or died, and the Pb treatment had no effect on the pregnancy duration. There was a significant decrease in maternal weight gain, brain, and placental weights in Pb-treated groups. However, this decrease was more marked in the Pb320 group as compared to the control group. Meanwhile, these effects improved with TQ co-treatment (Graph 1).



**Graph 1.** Effect of gestational Pb and TQ co-administration on pregnant rats' parameters (Mean ± SD) in different groups.

n = number of rats.  $P^1$ : compared to control.  $P^2$ : compared to TQ.  $P^3$ : compared to DMSO.  $P^4$ : compared to Pb160.  $P^5$ : compared to Pb320.

### Fetal results

The fetus from Pb-treated groups exhibited a reduction of fetal weight and fetal growth parameters, i.e. crown-rump length, head length, biparietal diameter, and umbilical cord length). This reduction was more marked in the Pb320-treated group as compared to the control. However, these effects improved with Pb320 + TQ cotreated group (Graph 2).

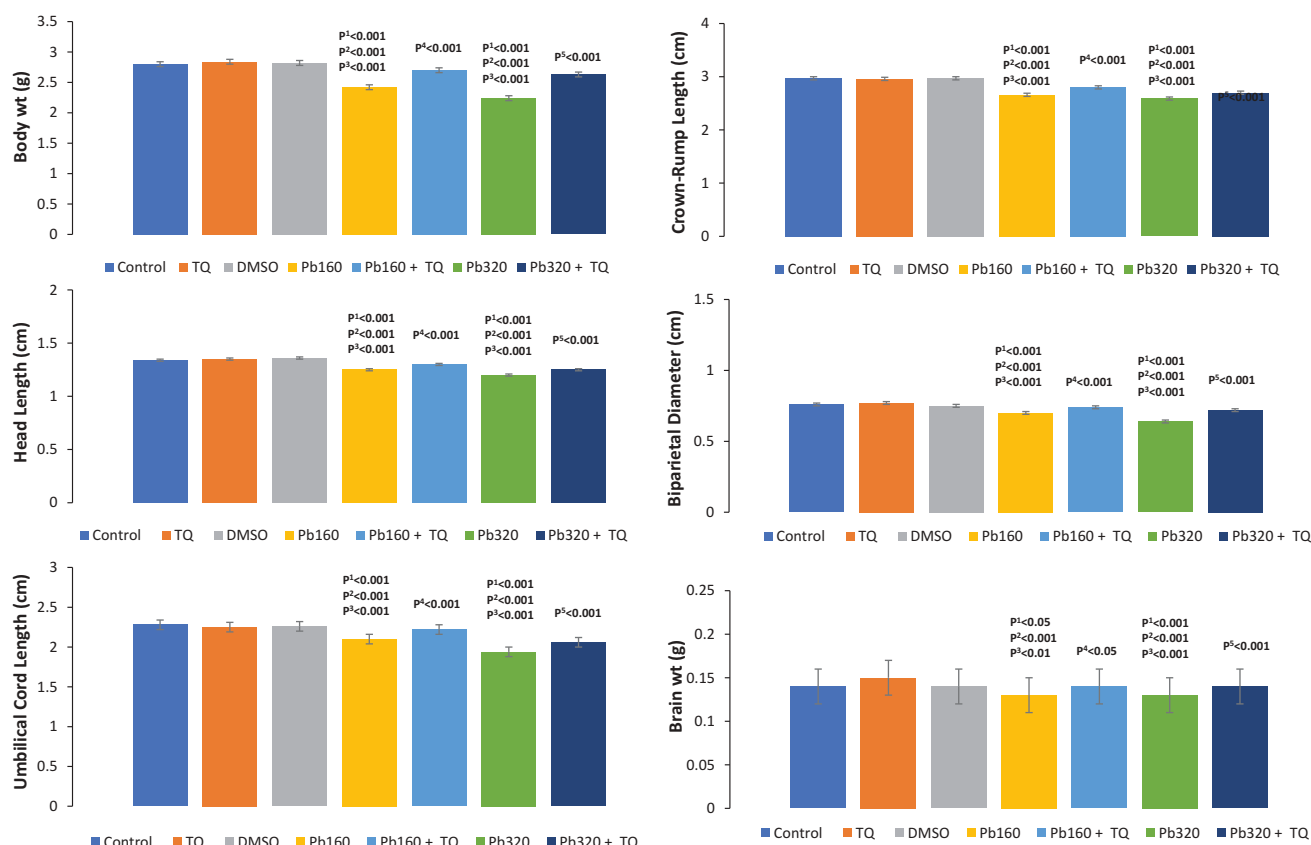
### Materno-fetal pb analysis

This analysis had significant increases in the mean values of Pb-level in the maternal blood, brains and fetal brains in Pb-treated groups than in the control especially in the Pb320 group. Also, TQ co-administration with Pb resulted in the reduction of Pb-levels as compared to the control, TQ, and DMSO groups. Lead content in the fetal brain was positively correlated to maternal Pb levels, which showed Pb had transferred from the mother to the fetus (Graph 3).

### Biochemical assays

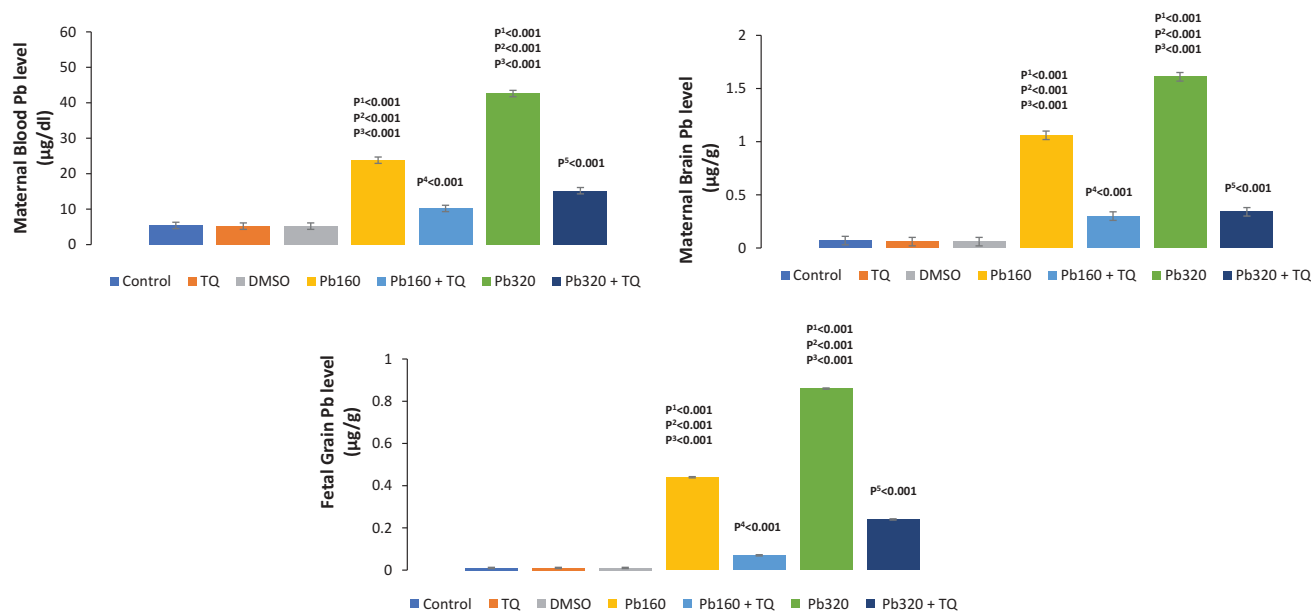
There was a significant increase of MDA level in the maternal brains of Pb-treated groups, which was significant as compared to control, TQ, and DMSO groups. Moreover, there was a decrease of the antioxidant enzymes, i.e. SOD, CAT, and GPx levels in Pb-treated groups (Pb160 & Pb320) in a dose-dependent manner, which was significant as compared to the control. TQ co-administration with Pb resulted in the decrease of MDA level and the increase of antioxidant enzyme levels, i.e. SOD, CAT, and GPx (Graph 4).





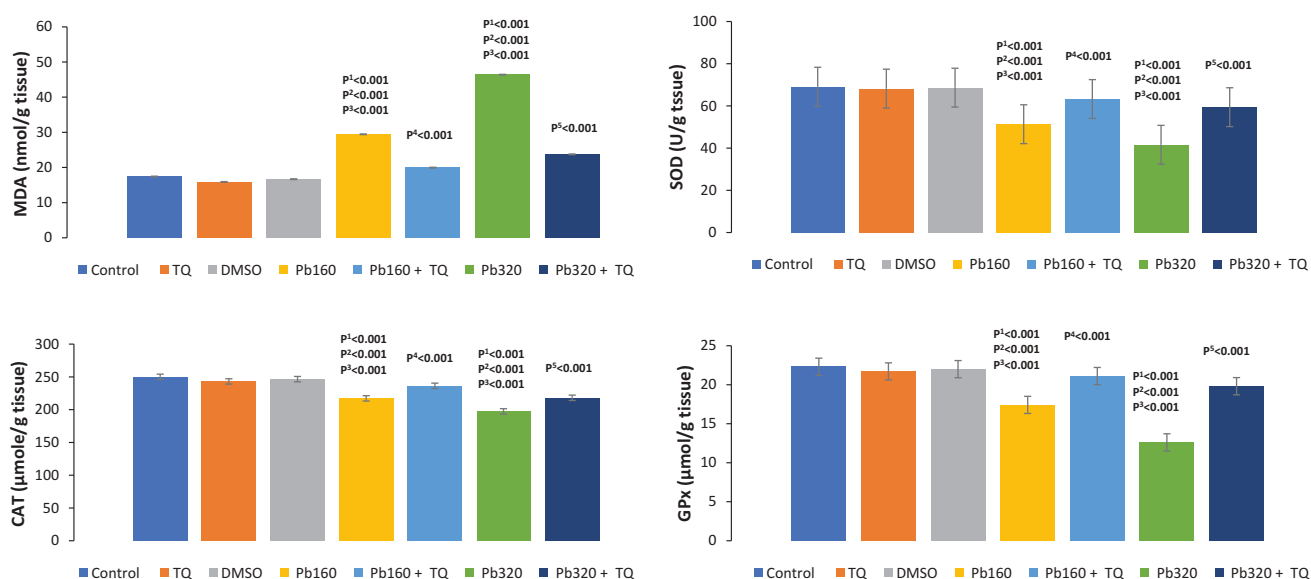
**Graph 2.** Effect of gestational Pb and TQ co-administration on fetal and brain weights and growth parameters (Mean  $\pm$  SD) in different groups.

n = number of rats. P<sup>1</sup>: compared to control. P<sup>2</sup>: compared to TQ. P<sup>3</sup>: compared to DMSO. P<sup>4</sup>: compared to Pb160. P<sup>5</sup>: compared to Pb320.



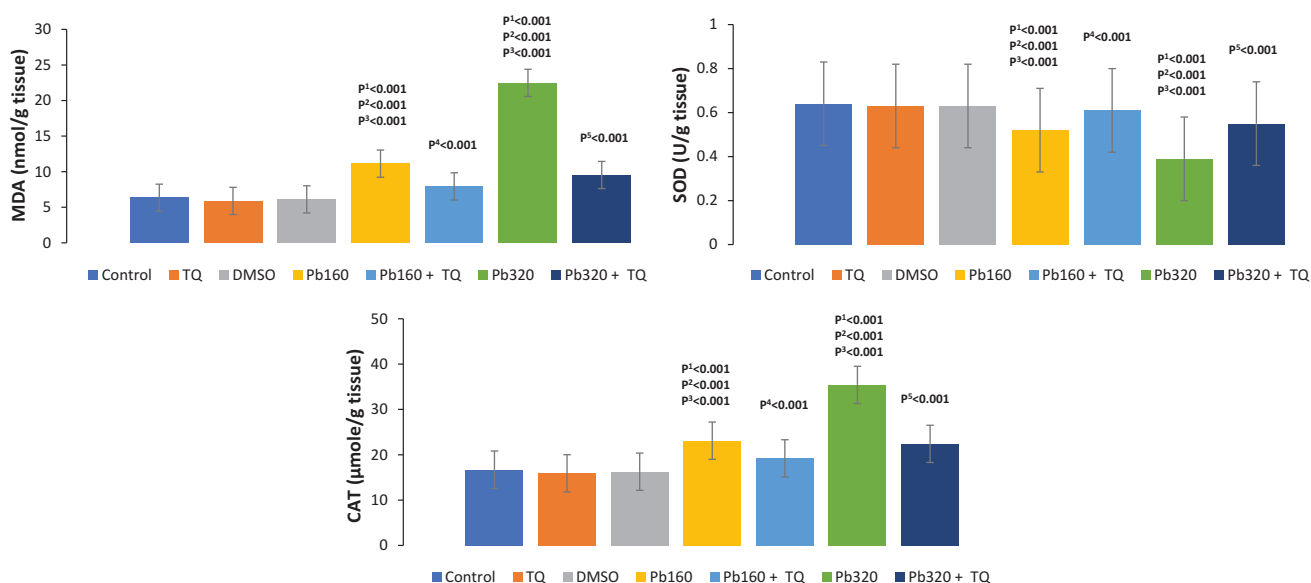
**Graph 3.** Effect of gestational Pb and TQ co-administration on maternal-fetal Pb concentrations (Mean  $\pm$  SD) in different groups.

n = number of rats. P<sup>1</sup>: compared to control. P<sup>2</sup>: compared to TQ. P<sup>3</sup>: compared to DMSO. P<sup>4</sup>: compared to Pb160. P<sup>5</sup>: compared to Pb320.



**Graph 4.** Effect of gestational Pb and TQ co-administration on the lipid peroxidation and antioxidant enzyme activities of the maternal brains (Mean  $\pm$  SD) in different groups.

n = number of rats. P<sup>1</sup>: compared to control. P<sup>2</sup>: compared to TQ. P<sup>3</sup>: compared to DMSO. P<sup>4</sup>: compared to Pb160. P<sup>5</sup>: compared to Pb320.



**Graph 5.** Effect of gestational Pb and TQ co-administration on the lipid peroxidation and antioxidant enzyme activities of the fetal brains (Mean  $\pm$  SD) in different groups.

n = number of rats. P<sup>1</sup>: compared to control. P<sup>2</sup>: compared to TQ. P<sup>3</sup>: compared to DMSO. P<sup>4</sup>: compared to Pb160. P<sup>5</sup>: compared to Pb320.

Regarding the fetal brains, there was a significant increase of MDA levels in the fetal brains of Pb-treated groups, which was significant as compared to the control, TQ, and DMSO groups, and the MDA level was higher in the Pb320 group. Furthermore, in Pb-treated groups, SOD, CAT, and GPx levels significantly decreased as compared to the control, TQ, and DMSO groups. These enzyme levels were lower in the Pb320 group. In contrast, TQ co-administration with

Pb was again dose-dependent with decreased MDA and increased antioxidant enzyme activities (Graph 5).

### Results for hematoxylin and eosin staining and GFAP immunostaining

#### Maternal brain

Microscopic examination of mother rat H&E stained sections showed similar histological findings in the control, TQ, and DMSO groups. In general, normal

morphology was seen in the six layers of the cerebral cortex (Figure 1a-c). In the Pb-treated groups, the examination revealed the variable degrees of change which were less evident in the Pb160 group (Figure 2 a,b) than in the Pb320 group (Figure 3 a,b). Disorganized cells and lack of characteristic, typical, layered structures were seen

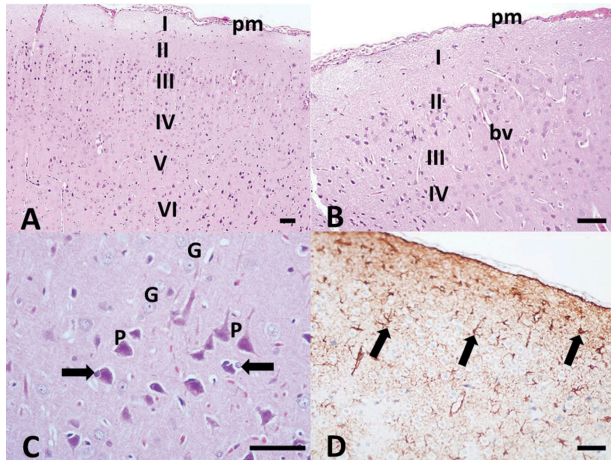


**Figure 1.** Photomicrographs of cerebral cortex from DIH<sub>2</sub>O control, TQ and DMSO treated mother rats (a, b) H&E shows normal layering pattern has six layers. I. Outer molecular layer, II. external granular layer; III. external pyramidal layer, IV. inner granular layer, V. inner pyramidal layer, VI. polymorphic layer. (c) H&E of pyramidal cells (P) have multipolar shape, vesicular nuclei, and basophilic cytoplasm while granular cells (G) have large nuclei, prominent nucleolus and little cytoplasm. Smaller neuroglia cells appear scattered (arrows). (d) Immunostaining for GFAP shows a few GFAP<sup>+</sup> astrocytes with brown cytoplasmic granules (arrows). Pia matter (pm); blood vessel (bv). Scale bar = 50  $\mu$ m.

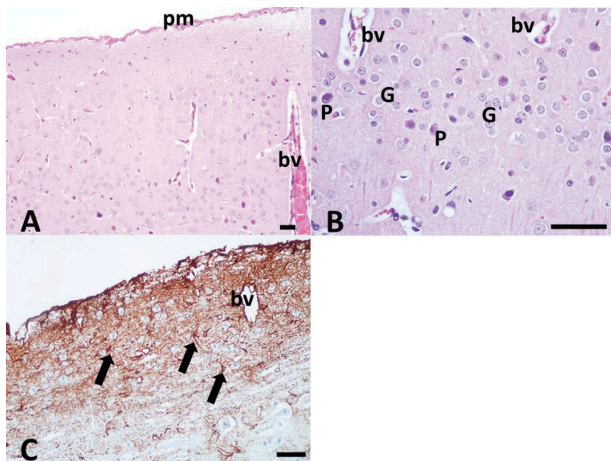


**Figure 2.** Photomicrographs of cerebral cortex from Pb160 mother rats (a) H&E shows some disorganized cortical layers (arrow) and congested blood vessels (bv). (b) H&E shows shrunken pyramidal cells (P) with loss of processes, dark cytoplasm and small darkly stained nucleus while granular cells (G) are surrounded by halos. (c) GFAP immunostaining shows increased GFAP<sup>+</sup> astrocytes (arrows) as compared to the control group. Pia (pm). Scale bar = 50  $\mu$ m.

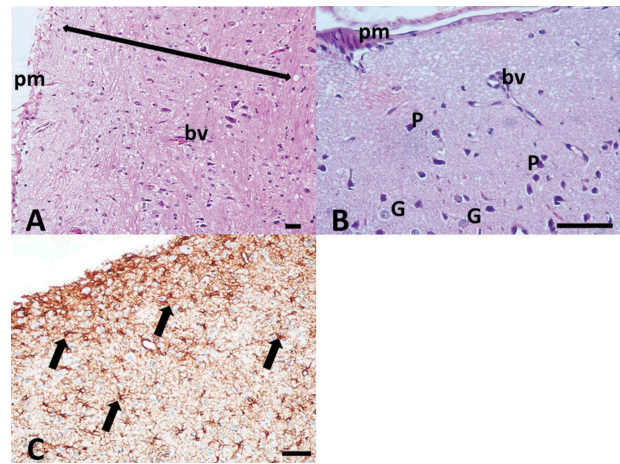


**Figure 3.** Photomicrographs of cerebral cortex from Pb320 mother rats (a) H&E shows distortion and disappearance of normally arranged cortical layers and dilated blood vessels (bv). (b) H&E shows darkly stained pyramidal cells (P) with irregular shape and pyknotic nuclei. Other cells have marked vacuolization with faintly stained cytoplasm. Note: some granular cells (G) are shrunken and deeply stained by H&E. (c) GFAP immunostaining shows a marked increase in the number of GFAP<sup>+</sup> astrocytes (arrows) as compared to low dose Pb treated and control groups. Pia matter (pm); blood vessel (bv). Scale bar = 50  $\mu$ m.

with some variable-sized vacuoles between cells. Some pyramidal cells appeared irregular in shape and darkly stained with loss of processes while other cells showed marked vacuolization with faintly stained cytoplasm. Most of granular cells were affected by ill-defined faint staining with pericellular halos. Also, some apoptotic cells with dense nuclei were observed. Regarding the Pb and TQ groups (Figure 4 a-c), there was improved histological

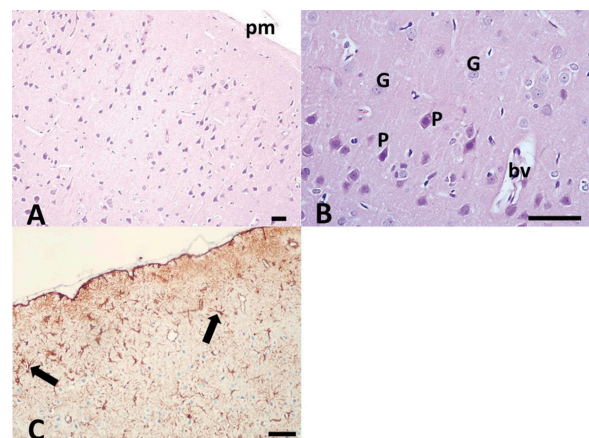


**Figure 4.** Photomicrographs of cerebral cortex from Pb and TQ-treated mother rats. (a) There is an improvement in histoarchitecture of organized layers in H&E. (b) Pyramidal cells (P) and granular cells (G) appear more normal in H&E section. (c) GFAP immunostaining shows a decreased number of GFAP<sup>+</sup> astrocytes as compared Pb-treated rats (in Figure 3) (arrows). Pia matter (pm), blood vessel (bv). Scale bar = 50  $\mu$ m.



appearance of the cortical layers, which appeared similar to the control, TQ, and DMSO groups in decreased cellular damage. The pyramidal cells appeared almost normal with vesicular nuclei, although some cells were still vacuolated with acidophilic cytoplasm.

Immunohistochemical staining for GFAP in cerebral cortex sections from control, TQ, and DMSO groups revealed few GFAP<sup>+</sup> astrocytes with their processes dispersed between the different cerebral cortex cell layers (Figure 1 d). In the Pb-treated groups, an increased number of GFAP<sup>+</sup> astrocytes was observed as compared to the control, TQ, and DMSO groups. This increase was greater in the Pb320 group (Figure 3 c) as compared to Pb160 group (Figure 2 c). In the Pb and TQ groups (Figure 4 c), there was a noticeable decrease in the GFAP<sup>+</sup> astrocytes as compared to the Pb-treated rats (Graph 6).

### Fetal brain

Microscopic examination of the H&E stained fetal brain sections from control, TQ and DMSO groups showed similar normal histological findings. The telencephalon wall formed a normal distinct structure consisting of five basic zones and a lateral ventricle (Figure 5 a). In the Pb160 group, the observation was similar with no difference from the control. In the Pb320 group (Figure 6 a), the examination of fetal brains revealed a lesser degree maturation as compared to the control fetuses with a dilated lateral ventricle as well as thinner, the unrecognizable arrangement of telencephalic wall layers. Moreover, there were thinner ventricular and subventricular zones, a widened intermediate zone and a reduced cortical zone. While fetal brains from the Pb- and TQ-groups (Figure 7 a), showed regressive changes, and the observation was similar to the control concerning the telencephalic wall thickness and lateral ventricle size.

Immunostaining for GFAP on fetal brain sections showed minimal GFAP<sup>+</sup> cellular reaction in the superficial layers of the telencephalic wall (Figure 5 b). The fetal brains from the Pb320 group had an apparent increase in the

number of GFAP<sup>+</sup> astrocytes as compared to the control, TQ and DMSO groups (Figure 6 b). However, a reduction of GFAP<sup>+</sup> astrocytes was observed in the fetal brain from Pb and TQ groups (Figure 7 b).

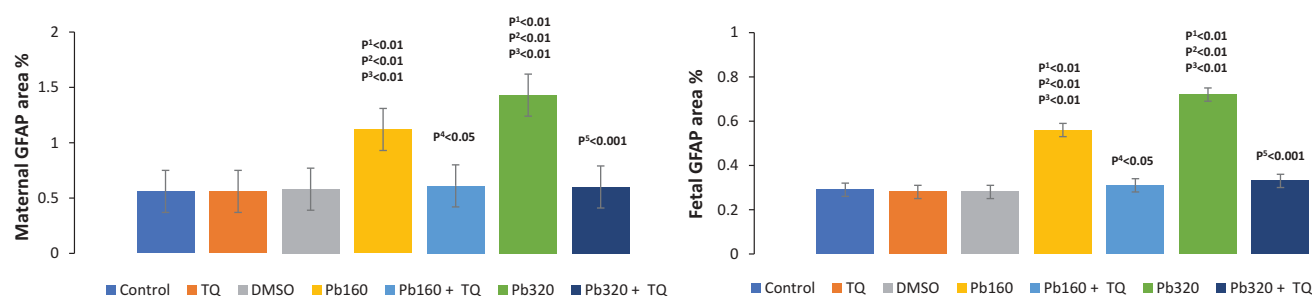
### Discussion

Nervous system is the primary target of Pb exposure, especially in the developing fetal brain. In the current study, Pb caused a significant reduction in brain weight, body weight in both mother and fetus as compared to control, which was obvious in the Pb320 group. In accordance, it was reported that Pb caused several adverse health effects that are dose-dependent and somewhat irreversible [29]. Also, it was found that Pb induces an important reduction in pup body and brain weight when their dams consumed 300 mg/L of Pb [9,30].

These results could be explained by the fact that Pb traverses the immature blood-brain barrier thus influencing the developing fetal brain growth and cellular proliferation [31,32]. Studies revealed that fetuses from pregnant mothers exposed to Pb level (0.01% and 0.05% w/v) exhibited higher fetal brain Pb levels [33].

Current results indicated that dam Pb exposure caused increased Pb concentrations in placental and fetal blood and the developing brain. Similarly, preceding studies showed highly concentrated Pb in the umbilical cord, placenta, and brain and supposed that the umbilical cord and placenta might be respectable biomarkers for fetal Pb-exposure [34]. Furthermore, another study demonstrated that Pb infiltrated the immature blood-brain barrier and accumulated in the fetal brain [35].

This current work found that Pb causes a significant increase in oxidative stress as evidenced by the high MDA level in the maternal and fetal brains. This was accompanied by a marked reduction of antioxidant enzymes (SOD, CAT, and GPx) in high and low Pb exposure groups. Another study found that a Pb-induced disturbance of the prooxidant/antioxidant balance in the brain



**Graph 6.** Area percentage of GFAP (Mean ± SD) in different groups.

n = number of rats. Percent area/cell is the product of percent area/(100× density). P<sup>1</sup>: compared to control. P<sup>2</sup>: compared to TQ. P<sup>3</sup>: compared to DMSO. P<sup>4</sup>: compared to Pb160. P<sup>5</sup>: compared to Pb320.

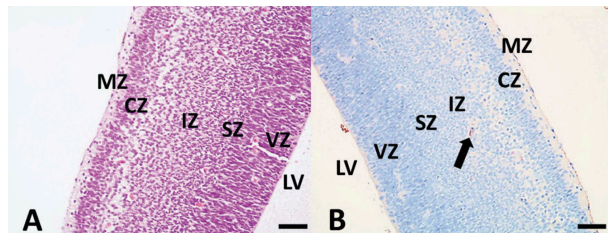


**Figure 5.** Photomicrographs of fetal brain at GD20 from control, TQ and DMSO treated group. (a) H&E section shows normal appearance of the telencephalic wall and lateral ventricle (LV). The telencephalic wall has five basic zones: marginal zone (MZ), cortical zone (CZ), intermediate zone (IZ), subventricular zone (SZ) and ventricular zone (VZ). (b) GFAP immunostaining shows few GFAP<sup>+</sup> cells scattered in the superficial telencephalic wall layers (arrow). Scale bar = 50 µm.

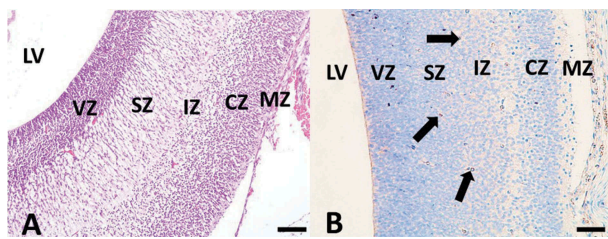


**Figure 6.** Photomicrographs of the fetal brain at GD20 from Pb320 group. (a) H&E section shows a thinner telencephalic wall with hardly detectable arrangement of the wall layers which have thinner ventricular (VZ) and subventricular (SZ) zones, wider intermediate zone (IZ), hypoplastic, narrower cortical zone (CZ) and disrupted marginal zone (MZ). (b) Immunostaining shows the GFAP<sup>+</sup> cells (arrows), are more scattered in the superficial telencephalic wall layers (SZ & IZ). Scale bar = 50 µm.

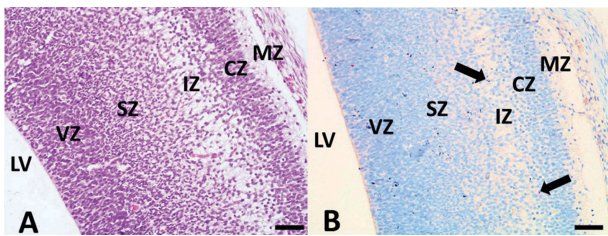


**Figure 7.** Photomicrographs of the fetal brain at GD20 from Pb320 and TQ-treated group. (a) H&E section shows normal appearance of the telencephalic wall with identifiable-arranged telencephalic wall layers, which appear similar to the DIH<sub>2</sub>O control fetal brain (Figure 5). (b) Immunostaining shows a reduced number of GFAP<sup>+</sup> astrocytes (arrows). Scale bar = 50 µm.

might encourage impairment to different cellular components, including nucleic acids, membrane lipids, and proteins [36]. Also, the Hassan group showed the MDA level was strongly correlated with Pb concentration in the brains of exposed rats [37]. Moreover, their results were consistent with earlier animal and human studies, which suggested that Pb exposure was associated with increased

oxidative stress and occurrence of neurotoxicity due to oxidative damages, as the brain consumes 20% of the body's oxygen [38].

Our results also showed increased oxidative stress in the fetal brains with pre-natal Pb-exposure. The toxic effects of Pb on the fetal brain are undoubtedly the main significant and meticulously studied outcome of intrauterine Pb-exposure [39]. Such effects might affect the behavior of young rat offspring, morphological developments and sensory motor reflexes of the pups [40].

Histopathology for the present study displayed a variable degree of morphological impairment of the maternal and fetal brains in both Pb-treated groups (Pb160 and Pb320), which was more understandable in animals exposed to the higher Pb dose. Pb-induced damage occurring in the cerebrum, hippocampus and cerebellum has affected various biological activities at the molecular, cellular, and intracellular levels and can cause morphological modifications in the brain which may persist after Pb levels drop [41]. In this study, there were decreased pyramidal cells along with the presence of degenerated cells with pyknotic nuclei in Pb-treated groups as compared to control. These findings agreed with a study which confirmed the direct effect of Pb on brain cells [42]. Correspondingly, Pb-induced cell death has been established in the cortex and cerebellum on neonatal rats (2–4 weeks old). This indicates a complex sensitivity in younger rats [32].

In the current study, increased GFAP<sup>+</sup> astrocytes detected in Pb-treated maternal brains could be attributed to hyper-reactivity of astrocytes against toxic effects of Pb and thus protecting neurons from these hazardous effects as reported by Chibowska et al. [42]. The mechanism explaining the increased GFAP<sup>+</sup> astrocytes in the neonatal brain after maternal Pb intake detected in this study might be attributed to a role in modulating astrogliosis. The observed gliosis in Pb-treated groups could be caused by the ROS formation and reduced antioxidants [28]. Thus, GFAP marker detection by IHC may be the appropriate test to determine neurodegenerative impairments [28]. Regarding the fetal brains in this study, few GFAP<sup>+</sup> astrocytes were seen in the cortex.

Co-administration of TQ with Pb to mother rats in this study produced a significant improvement in the histopathological findings in maternal and fetal brains, which appeared similar to the control, especially in the Pb160 group. Studies also reported that TQ has great potential for the prevention of multiple neurological conditions and improved brain lesions resulting from Parkinson's disease [43] and status epilepticus [44]. Moreover, recent studies have described the neuropharmacological properties of TQ in designed neurological models where it was found that TQ prevented

the brain damage in a chronic toluene-induced neurodegeneration model in the hippocampus and transient forebrain ischemia [45].

In the present study, TQ co-treatment with Pb resulted in an improvement of different oxidative parameters in the maternal and fetal brains, i.e. MDA, SOD, CAT, and GPx. Similarly, it was reported that TQ was well known to have antioxidant properties [16] and also found it prevented lipid peroxidation during cerebral ischemia-reperfusion injury in rat hippocampus [24]. TQ is also a potent free radical scavenger that conserves the activity of several antioxidant enzymes, such as glutathione-S-transferase, glutathione peroxidase, and catalase. Also, and in agreement to our results, Farkhondeh and colleagues also found that TQ reduced the cerebral oxidative injuries induced by Pb and ionizing radiation [46].

## Conclusion

This study is important in providing evidence of the beneficial role of TQ as a natural antioxidant in the protection against maternal and fetal Pb neurotoxicity through the reduction of oxidative stress and reversibility of the histopathological changes. Finally, efforts with active steps should be taken towards the prevention of lead occupational and household exposure, i.e. lead paint, lead pipes, and mining waste.

## Acknowledgments

The authors, therefore, acknowledge with thanks to DSR technical and financial support.

## Disclosure statement

No potential conflict of interest was reported by the authors.

## Funding

This work was supported by the Deanship of Scientific Research, King Abdulaziz University, Jeddah, Saudi Arabia [RG/04/32].

## Notes on contributors

**Hamid A Saleh**, PhD is an Associate Professor in the Anatomy Department, Faculty of Medicine, King Abdulaziz University, Jeddah, Saudi Arabia.

**Gamal S. Abd El-Aziz**, MD is an Associate Professor in the Anatomy Department, Faculty of Medicine, King Abdulaziz University, Jeddah, Saudi Arabia.

**Hesham N. Mustafa**, MD is an Associate Professor in Basic Medical Sciences (Anatomy) department and coordinator of

Anatomy in Faculty of Dentistry. He is a member of European Society for the Study of Peripheral Nerve Repair and Regeneration (ESPNR); the Institute of Research Engineers and Doctors (IRED); Curriculum Development Committee of First phase for the academic years in the Faculty of Medicine. He serves as a reviewer for many reputed ISI-indexed journals. He has given the Award of Excellence of Scientific Publication for staff members, from Deanship of Scientific Research, King Abdulaziz University, Jeddah, Saudi Arabia the Certificate for Highly Cited Paper from Elsevier in December, 2016, and was Publons Top reviewer (1%) for Pharmacology and Toxicology and Clinical Medicine in September 2018.

**Magdy El-Fark**, MD is an Associate Professor in the Anatomy Department, Faculty of Medicine, Suez Canal University, Ismailia, Egypt.

**Majdah Aburas**, PhD is an Assistant Professor in the Biology Department, Faculty of Science and Ahmed Othman Mal, PhD is an Associate Professor on the Faculty of Marine Sciences, at King Abdulaziz University, Jeddah, Saudi Arabia.

**Abdel Halim Deifalla**, Salem, MD is a Professor in the Anatomy Department, Faculty of Medicine, Arabian Gulf University, Bahrain.

## ORCID

Hamid A Saleh  <http://orcid.org/0000-0003-1374-8862>

Gamal S. Abd El-Aziz  <http://orcid.org/0000-0003-0398-0297>

Hesham N. Mustafa  <http://orcid.org/0000-0003-1188-2187>

## References

- [1] Grandjean P, Bellinger D, Bergman A, et al. The faroes statement: human health effects of developmental exposure to chemicals in our environment. *Basic Clin Pharmacol Toxicol.* **2008**;102(2):73–75.
- [2] Flora G, Gupta D, Tiwari A. Toxicity of lead: a review with recent updates. *Interdiscip Toxicol.* **2012**;5(2):47–58.
- [3] Cory-Slechta DA, Virgolini MB, Rossi-George A, et al. Lifetime consequences of combined maternal lead and stress. *Basic Clin Pharmacol Toxicol.* **2008**;102(2):218–227.
- [4] Sanders T, Liu Y, Buchner V, et al. Neurotoxic effects and biomarkers of lead exposure: a review. *Rev Environ Health.* **2009**;24(1):15–45.
- [5] Liu J, Han D, Li Y, et al. Lead affects apoptosis and related gene XIAP and Smac expression in the hippocampus of developing rats. *Neurochem Res.* **2010**;35(3):473–479.
- [6] Bokara KK, Brown E, McCormick R, et al. Lead-induced increase in antioxidant enzymes and lipid peroxidation products in developing rat brain. *Biometals.* **2008**;21(1):9–16.
- [7] Bokara KK, Blaylock I, Denise SB, et al. Influence of lead acetate on glutathione and its related enzymes in different regions of rat brain. *J Appl Toxicol.* **2009**;29(5):452–458.



- [8] Posser T, de Aguiar CBNM, Garcez RC, et al. Exposure of C6 glioma cells to Pb(II) increases the phosphorylation of p38MAPK and JNK1/2 but not of ERK1/2. *Arch Toxicol.* **2007**;81(6):407–414.
- [9] Ashafaq M, Tabassum H, Vishnoi S, et al. Tannic acid alleviates lead acetate-induced neurochemical perturbations in rat brain. *Neurosci Lett.* **2016**;617:94–100.
- [10] Taborsky J, Kunt M, Kloucek P, et al. Identification of potential sources of thymoquinone and related compounds in Asteraceae, Cupressaceae, Lamiaceae, and Ranunculaceae families. *Cent Eur J Chem.* **2012**; 10(6):1899–1906.
- [11] Farooqui Z, Ahmed F, Rizwan S, et al. Protective effect of *Nigella sativa* oil on cisplatin induced nephrotoxicity and oxidative damage in rat kidney. *Biomed Pharmacother.* **2017**;85:7–15.
- [12] Barkat MA, Harshita, Ahmad J, et al. Insights into the targeting potential of thymoquinone for therapeutic intervention against triple-negative breast cancer. *Curr Drug Targets.* **2018**;19(1):70–80.
- [13] Ozer EK, Goktas MT, Toker A, et al. Thymoquinone protects against the sepsis induced mortality, mesenteric hypoperfusion, aortic dysfunction and multiple organ damage in rats. *Pharmacol Rep.* **2017**;69(4):683–690.
- [14] Ustyoğlu L, Demirören K, Kandemir I, et al. Comparative nephroprotective effects of silymarin, N-acetylcysteine, and thymoquinone against carbon tetrachloride-induced nephrotoxicity in rats. *Iran Red Crescent MedJ.* **2017**;19(1):e37746.
- [15] Hosseini S, Rad AK, Bideskan AE, et al. Thymoquinone ameliorates renal damage in unilateral ureteral obstruction in rats. *Pharmacol Rep.* **2017**; 69(4):648–657.
- [16] Khalilullah H. Anti-epileptic action of thymoquinone in Molecular and Therapeutic: actions of Thymoquinone. Younnus H, editor. Singapore: Springer; **2018**. p. 75–80.
- [17] Amin B, Hosseinzadeh H. Black Cumin (*Nigella sativa*) and its active constituent, thymoquinone: an overview on the analgesic and anti-inflammatory effects. *Planta Med.* **2016**;82(1–2):8–16.
- [18] Elkhayat ES, Alorainy MS, El-Ashmawy IM, et al. Potential antidepressant constituents of *Nigella sativa* seeds. *Pharmacogn Mag.* **2016**;12(1):S27–31.
- [19] Khan RA, Najmi AK, Khuroo AH, et al. Ameliorating effects of thymoquinone in rodent models of schizophrenia. *Afr J Pharm Pharmacol.* **2014**;8(15): 413–421.
- [20] Sayeed MSB, Asaduzzaman M, Morshed H, et al. The effect of *Nigella sativa* Linn. seed on memory, attention and cognition in healthy human volunteers. *J Ethnopharmacol.* **2013**;148(3):780–786.
- [21] Chen L, Li B, Chen B, et al. Thymoquinone alleviates the experimental diabetic peripheral neuropathy by modulation of inflammation. *Sci Rep.* **2016**;6:31656.
- [22] Adu EK, Yeboah S. The efficacy of the vaginal plug formation after mating for pregnancy diagnosis, and embryonic resorption in utero in the greater cane rat (*Thryonomys swinderianus*, Temminck). *Trop Anim Health Prod.* **2000**;32(1):1–10.
- [23] Villeda-Hernandez J, Mendez Armenta M, Barroso-Moguel R, et al. Morphometric analysis of brain lesions in rat fetuses prenatally exposed to low-level lead acetate: correlation with lipid peroxidation. *Histol Histopathol.* **2006**;21(6):609–617.
- [24] Kassab RB, El-Hennamy RE. The role of thymoquinone as a potent antioxidant in ameliorating the neurotoxic effect of sodium arsenate in female rat. *Egypt J Basic Appl Sci.* **2017**;4(3):160–167.
- [25] Sepehri H, Ganji F. The protective role of ascorbic acid on hippocampal CA1 pyramidal neurons in a rat model of maternal lead exposure. *J Chem Neuroanat.* **2016**;74(C):5–10.
- [26] Mustafa HN, Hegazy GA, Awdan SAE, et al. Protective role of CoQ10 or L-carnitine on the integrity of the myocardium in doxorubicin induced toxicity. *Tissue Cell.* **2017**;49(3):410–426.
- [27] Mustafa HN, El Awdan SA, Hegazy GA, et al. Prophylactic role of coenzyme Q10 and *Cynara scolymus* L on doxorubicin-induced toxicity in rats: biochemical and immunohistochemical study. *Indian J Pharmacol.* **2015**;47(6):649–656.
- [28] Mustafa HN, Hussein AM. Does allicin combined with vitamin B-complex have superior potentials than alpha-tocopherol alone in ameliorating lead acetate-induced Purkinje cell alterations in rats? An immunohistochemical and ultrastructural study. *Folia Morphol (Warsz).* **2016**;75(1):76–86.
- [29] Wang Y, Wang S. Effects of lead exposure on histological structure and antioxidant capacity in the cerebellum of 30-day-old mice. *Neural Regen Res.* **2011**; 6(14):1077–1081.
- [30] Attia AM, Ibrahim FA, Nabil GM, et al. Antioxidant effects of ginger (*Zingiber officinale* Roscoe) against lead acetate-induced hepatotoxicity in rats. *Afr J Pharm Pharmacol.* **2013**;7(20):1213–1219.
- [31] Yang J, Song S, Li J, et al. Neuroprotective effect of curcumin on hippocampal injury in 6-OHDA-induced Parkinson's disease rat. *Pathol Res Pract.* **2014**; 210(6):357–362.
- [32] Chang BJ, Jang BJ, Son TG, et al. Ascorbic acid ameliorates oxidative damage induced by maternal low-level lead exposure in the hippocampus of rat pups during gestation and lactation. *Food Chem Toxicol.* **2012**;50(2):104–108.
- [33] Dribben WH, Creeley CE, Farber N. Low-level lead exposure triggers neuronal apoptosis in the developing mouse brain. *Neurotoxicol Teratol.* **2011**;33(4):473–480.
- [34] Hamed EA, Meki AR, Abd El-Mottaleb NA. Protective effect of green tea on lead-induced oxidative damage in rat's blood and brain tissue homogenates. *J Physiol Biochem.* **2010**;66(2):143–151.
- [35] Flora SJ, Gautam P, Kushwaha P. Lead and ethanol co-exposure lead to blood oxidative stress and subsequent neuronal apoptosis in rats. *Alcohol Alcohol.* **2012**;47(2):92–101.
- [36] Dalia M. Effect of using pectin on lead toxicity. *J Am Sci.* **2010**;6(12):541–554.
- [37] Hassan A, Jassim H. Effect of treating lactating rats with lead acetate and its interaction with vitamin E or C on neurobehavior, development and some biochemical parameters in their pups. *Iraqi J Vet Sci.* **2010**; 24(1):45–52.
- [38] Abdel Moneim AE. Flaxseed oil as a neuroprotective agent on lead acetate-induced monoaminergic alterations



- and neurotoxicity in rats. *Biol Trace Elem Res.* **2012**; 148(3):363–370.
- [39] Sadek K. Barley phenolic compounds impedes oxidative stress in lead acetate intoxicated rabbits. *Oxid Antioxid Med Sci.* **2012**;1(2):141–146.
- [40] Benammi H, Erazi H, El Hiba O, et al. Disturbed sensorimotor and electrophysiological patterns in lead intoxicated rats during development are restored by curcumin I. *PLoS One.* **2017**;12(3):e0172715.
- [41] Chen JJ, Dai L, Zhao LX, et al. Intrathecal curcumin attenuates pain hypersensitivity and decreases spinal neuroinflammation in rat model of monoarthritis. *Sci Rep.* **2015**;5:10278.
- [42] Chibowska K, Baranowska-Bosiacka I, Falkowska A, et al. Effect of Lead (Pb) on Inflammatory Processes in the Brain. *Int J Mol Sci.* **2016**;17(12):2140.
- [43] Ebrahimi SS, Oryan S, Izadpanah E, et al. Thymoquinone exerts neuroprotective effect in animal model of Parkinson's disease. *Toxicol Lett.* **2017**;276:108–114.
- [44] Shao Y, Feng Y, Xie Y, et al. Protective effects of thymoquinone against convulsant activity induced by lithium-pilocarpine in a model of status epilepticus. *Neurochem Res.* **2016**;41(12):3399–3406.
- [45] Gokce EC, Kahveci R, Gokce A, et al. Neuroprotective effects of thymoquinone against spinal cord ischemia-reperfusion injury by attenuation of inflammation, oxidative stress, and apoptosis. *J Neurosurg Spine.* **2016**;24(6):949–959.
- [46] Farkhondeh T, Samarghandian S, Shahri AMP, et al. The neuroprotective effects of thymoquinone: a review. *Dose Response.* **2018**;16(2):1559325818761455.